Special Collection

Exploring the Full Potential of Photocatalytic Carbon Dioxide Reduction Using a Dinuclear Re_2Cl_2 Complex Assisted by Various Photosensitizers

Robin Giereth,[a, b] Martin Obermeier,[c] Lukas Forschner,[a] Michael Karnahl,[d] Matthias Schwalbe,*[c] and Stefanie Tschierlei*[a, b]

Photosensitizing units have already been applied to enable light-driven catalytic reduction of CO_2 with mononuclear rhenium complexes. However, dinuclear catalytic systems that are able to activate CO_2 in a cooperative bimetallic fashion have only rarely been combined with photosensitizers. We here present detailed studies on the influence of additional photosensitizers on the catalytic performance of a dirhenium complex (**Re_2Cl_2**) and present correlations with spectroscopic measurements, which shed light on the reaction mechanism. The use of [Ir(dFppy)$_3$] (**Ir**, dFppy = 2-(4,6-difluorophenyl)pyridine)) resulted in considerably faster CO_2 to CO transformation than [Cu(xant)(bcp)]PF_6 (**Cu**, xant = xantphos, bcp = bathocuproine). Emission quenching studies, transient absorption as well as IR spectroscopy provide information about the electron transfer paths of the intermolecular systems. It turned out that formation of double reduced species **$[Re_2Cl_2]^{2-}$** along with an intermediate with a Re–Re bond (**[ReRe]**) can be taken as an indication of multi-electron storage capacity. Furthermore, under catalytic conditions a CO_2-bridged intermediate was identified.

1. Introduction

Dinuclear metal catalysts with a specifically chosen ligand environment and orientation of the metal centers bear a high potential for effective bimetallic activation of CO_2 by cooperative effects.[1–3] The (cooperative) activation of small molecules is of particular importance for solar fuel production, considering the fact that usually several redox equivalents are required in order to overcome thermodynamically unfavored stepwise monoelectronic pathways.[4–7] Various design motifs for multi-electron storage in solar energy conversion schemes have been developed over the years, including dinuclear rhodium complexes,[8–15] or a multi-electron chargeable cobalt porphyrin catalyst.[16]

Bimetallic activation of CO_2 was recently reported by Jurss *et al.* in electrocatalytic studies on an anthracene-bridged dinuclear rhenium complex.[17] However, bimetallic activation was not observed under photocatalytic conditions.[18] In a recent study we explored a rather unexpected wavelength dependency of the well-known mononuclear complex [Re(bpy)(CO)$_3$Cl] (**bpy-Re**, with bpy = 2,2′-bipyridine) during photocatalysis.[19] It was found that particularly the Re–Re bonded dimer [Re(bpy)(CO)$_3$]$_2$ is a crucial intermediate, or better resting state.[19] We therefore synthesized and thoroughly characterized a new xanthene-bridged dinuclear **Re_2Cl_2** complex, where special attention was given to the spatial orientation of the two Re(bpy)(CO)$_3$Cl units.[20] Two isomers, *cis* and *trans*, were synthesized and only latter (shown in Scheme 1) investigated in more detail due to possible interconversion of the *cis* to the *trans* isomer. Although

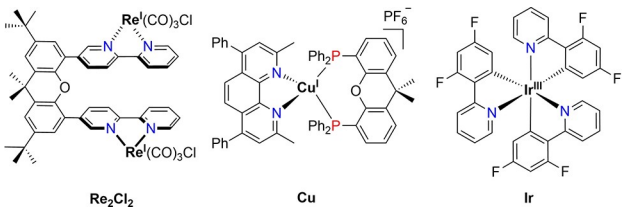

Re_2Cl_2 **Cu** **Ir**

Scheme 1. Structures and abbreviations of the dinuclear Re^{I} complex **Re_2Cl_2** and photosensitizers **Cu** ([Cu(xant)(bcp)]$^+$, xant = xantphos, bcp = bathocuproine) and **Ir** ([Ir(dFppy)$_3$], dFppy = 2-(4,6-difluorophenyl)pyridine).

[a] R. Giereth, L. Forschner, Prof. Dr. S. Tschierlei
Institute of Inorganic Chemistry I
Ulm University
Albert-Einstein-Allee 11, 89081 Ulm (Germany)
[b] R. Giereth, Prof. Dr. S. Tschierlei
Department of Energy Conversion
Institute of Physical and Theoretical Chemistry
Technische Universität Braunschweig
Gaußstr. 17, 38106 Braunschweig (Germany)
E-mail: s.tschierlei@tu-bs.de
[c] M. Obermeier, Dr. M. Schwalbe
Institute of Chemistry
Humboldt-Universität zu Berlin
Brook-Taylor-Str. 2, 12489 Berlin (Germany)
E-mail: matthias.schwalbe@hu-berlin.de
[d] Dr. M. Karnahl
Institute of Organic Chemistry
University of Stuttgart
Pfaffenwaldring 55, 70569 Stuttgart (Germany)

Supporting information for this article is available on the WWW under https://doi.org/10.1002/cptc.202100034

An invited contribution to a Special Collection on Photocatalytic CO_2 Reduction.

increased photo- as well as electrocatalytic activity compared to mononuclear **bpy-Re** was observed, the full potential of $\mathbf{Re_2Cl_2}$ (always referring to the *trans* isomer in the following) in photocatalysis could not fully be exploited yet.

Initial studies revealed that the accumulation of two electrons on $\mathbf{Re_2Cl_2}$ by photoinduced electron transfer reactions from sacrificial electron donors is hampered by a strong electronic communication between the two metal fragments.[20] However, if the system was reduced twice (*e.g.* by electrochemical reduction), a cooperative behavior was observed, as evidenced by a considerably lowered onset potential for electrocatalysis.

There are numerous references in which the addition of photosensitizers is used to increase the light harvesting properties or enable photo-activation of rhenium-based CO_2 reduction catalysts in the visible spectral window by providing highly potent reduction equivalents.[21–30] Many examples consist of the combination of a Ru^{II} based photosensitizer and a catalytic subunit in supramolecular assemblies. Hereby, Ru^{II} based chromophores, such as $[Ru^{II}(R_2\text{-bpy})_3]^{2+}$ (R=H, Me), were shown to increase the catalytic activity of **bpy-Re** in an intermolecular system up to $TON_{CO} = 170$ from $TON_{CO} \sim 30$ without photosensitizer.[21,30] An even more efficient system was received by exchanging the catalyst with a Re^{I} diimine biscarbonyl bisphosphine unit, whereby a $TON_{CO} = 3029$ was obtained.[31] However, thermodynamic constraints are still a bottleneck for an efficient electron transfer from photoreduced Ru^{II} complexes to Re^{I} units.[21,29,30,32,33] In other cases Ir^{III} based chromophores have been utilized. In a prominent example, a Ir^{III} 1-phenylisoquinoline complex was employed as a photosensitizing unit in combination with *fac*-Re(dmb)$(CO)_3$Br (dmb = 4,4′-dimethyl-2,2′-bipyridine). Interestingly, the increase in activity was the same, regardless if used in an inter- or supramolecular system.[34]

Intermolecular photosensitization using environmentally benign photosensitizer (PS), for example, $[Cu(xant)(bcp)]^+$ (**Cu**, see also Scheme 1) has only recently been exploited in the photocatalytic CO_2 to CO reduction.[35–40] Exemplarily, **Cu** in combination with Re(bpy)$(CO)_3$Br as catalyst[37] increased the catalytic activity (TON_{CO}) by a factor of ~6 from 40 to 240 after 1 h illumination with $h\nu > 370$ nm (optimized conditions: [Re] = 0.05 mM, [BIH] = 0.1 M, [Cu] = 0.5 mM, in DMF-TEOA (4:1, *v/v*)).

We, thus, envisioned the utilization of an external/additional stimulus, *i.e.* photosensitizer (PS), in order to achieve higher reduced states of $\mathbf{Re_2Cl_2}$. Hence, herein, results to elucidate the influence of external PS to enhance the catalytic activity for CO_2 reduction by a potential cooperative activation pathway are presented. To the best of our knowledge, this method of photosensitization has not been used to exploit bimetallic activation of CO_2 with dinuclear rhenium catalysts, yet. Possible two electron transfer processes are investigated by spectro-electrochemical and chemical reduction experiments, and multi-electron storage properties are tested.

2. Results and Discussion

2.1. Photocatalytic Studies

Compound $\mathbf{Re_2Cl_2}$ was synthesized according to an already published method.[20] As outlined in the introduction, the goal of the recent studies is to achieve an efficient and fast formation of higher reduced species of $\mathbf{Re_2Cl_2}$, *i.e.* $[\mathbf{Re_2Cl_2}]^{n-}$. Since the prerequisite for the formation of doubly-reduced $\mathbf{Re_2Cl_2}$ by an external photosensitizer is a) a high reductive power in the ground-state (*c.f.* $E < -1.85$ V vs. Fc/Fc^+, Table 1) and b) a high oxidative power in the excited-state (*i.e.* reductive quenching by sacrificial electron donors should be feasible), only few photosensitizers can be considered (Table 1). Especially **Ir** and **Cu** (Scheme 1) do match these conditions and were chosen for further catalytic experiments.[41–43] As sacrificial reductants either triethylamine (TEA), triethanolamine (TEOA) or 1,3-dimethyl-2-phenylbenz-imidazoline (BIH), or a combination of these (*vide infra*) were selected.[44] In earlier studies, TEOA was used in most cases.[19,45,46] However, TEOA induces competitive and in our case unwanted side reactions during the formation of the catalytically active species (*vide infra*).[47] Besides, TEA is a better base than TEOA to deprotonate $BIH^{\bullet+}$, which is the product of the reductive quenching of PS with BIH, and thus, prevents fast back electron transfer from $BIH^{\bullet+}$ to reduced $[PS]^-$ as described by Sampaio *et al.*[48]

Initial experiments, applying a $\lambda > 400$ nm longpass filter, confirmed these statements: *I.e.* without BIH and only using a DMF/TEOA (20 vol%) mixture a $TON_{CO,24h}$ of 10 is reached that is much lower than a $TON_{CO,4h}$ of 52 (entry 1, Table 2) obtained

Table 1. Ground and excited state redox potentials [V] and MLCT absorption maxima [nm] with corresponding molar attenuation coefficients ε [10^3 $M^{-1}cm^{-1}$] of $\mathbf{Re_2Cl_2}$ and photosensitizers **Cu** and **Ir** as well as oxidation potentials of sacrificial reductants TEA, TEOA and BIH. Additionally, redox potentials and absorption maxima of reaction intermediates of $\mathbf{Re_2Cl_2}$ are given. Peak potentials are given vs. Fc/Fc^+.

Compound	E_{red}	E_{ox}	E_{red}*	E_{ox}*	λ_{abs} (ε)	Ref.
$\mathbf{Re_2Cl_2}$	−1.71	+0.99	+0.77	−1.49	365 (15.5)	20
$[\mathbf{Re_2Cl_2}]^{1-}$	−1.85	−1.61			580 (16.7)	20
[ReRe]	~−1.9[a]	−0.46			810	20
Cu	−2.05	+0.93	+0.63	−1.75	389 (5.1)	49
Ir[b,c]	−2.38	+0.91	+0.37	−1.84	379 (7.1)	41, 50
TEA		+0.31 ± 0.46				44, 49
BIH		−0.05				44
TEOA		+0.19 ± 0.44				44, 51

[a] calculated; [b] *fac*-isomer; [c] redox potentials $E_{1/2}$.

Table 2. $TON_{CO,max}$ (reached after around 4 h reaction time) of Re_2Cl_2 (always 50 μM) in DMF in relation to various ratios of electron donor (TEA or TEA/BIH) and photosensitizers (**Ir** or **Cu**). A cut-off filter with hν > 400 nm was used for all measurements due to the low absorptivity of the photosensitizers in the visible region and to avoid detrimental UV light.

Entry	PS	BIH [eq.]	TEA [eq.]	PS [eq.]	$TON_{CO,max}$
1	**Ir**	–	5 % (*v/v*)	1	52
2	**Ir**	100	100	1	78
3	**Ir**	200	200	1	195
3a[a]	**Ir**	200	200	1	154
4[a]	**Ir**	200	400	1	131
5[a]	**Ir**	400	200	1	134
6[a]	**Ir**	400	400	1	193
7[a]	**Ir**	1000	1000	1	255
8	–	200	200	–	63[b]
9	**Ir**	200	200	0.1	124
10	**Ir**	200	200	0.25	144
11	**Ir**	200	200	0.5	149
12	**Ir**	1000	1000	2	270
13	**Cu**	200	200	1	169[b]

[a] Lower quality batch of BIH was used; [b] TON_{CO} after 4 h, but catalysis still continues.

using only DMF/TEA (5 vol %). When using 200 eq. BIH in combination with DMF/TEOA (20 vol %) a $TON_{CO,24h}$ of 49 is reached that can be increased to a $TON_{CO,24h}$ of 200 when using 2000 eq. BIH.[20] On the other hand, using 200 eq. BIH/200 eq. TEA in DMF a $TON_{CO,4h}$ of 63 (green trace, Figure 1) and $TON_{CO,24h}$ of 109 is determined. (Please note, that a $TON_{CO,max}$ means that the final point of catalytic transformation is reached, while a time indication means that the catalyst is still active after the specified time point.) As we see a lower TON_{CO} when using BIH/TEOA instead of BIH/TEA mixtures, in most of the following experiments TEA was applied as base. Please note that in no experiment the formation of hydrogen or formic acid could be determined (see further details in SI).

The addition of an external photosensitizer should accelerate the formation of CO. However, the $TON_{CO,max}$ value when **Ir** is used as PS in DMF/TEA (5 vol %) is identical to the reaction without PS (black and red curve in Figure 1), because TEA is not able to quench the excited state of **Ir** (*vide infra*). On the contrary, using **Ir** and BIH/TEA (both 200 eq.) an increase of the $TON_{CO,max}$ by a factor of ~4 is observed giving quantitative formation of CO after 2 h reaction time, i.e. $TON_{CO,max}$ of 195 (blue curve in Figure 1). Please note that after two hours of illumination using BIH/TEA (both 200 eq.) but without additional PS (green trace, Figure 1), only a $TON_{CO,2h}$ of 28 is reached. The usage of BIH/TEOA (both 200 eq.) again leads to lower catalytic performance and only a $TON_{CO,max}$ of 122 is reached (orange curve in Figure 1). Surprisingly, while Re_2Cl_2 without PS still shows catalytic activity after 24 hours of illumination, the $TON_{CO,max}$ when **Ir** is involved is already reached after 2 hours reaction time (compare blue and red curve in Figure 1 to green curve). Nevertheless, the usage of **Ir** instead of **Cu** is advantageous, because a slower CO_2 to CO reduction is observed in case of **Cu** and a $TON_{CO,4h} = 169$ is determined (magenta curve in Figure 1).

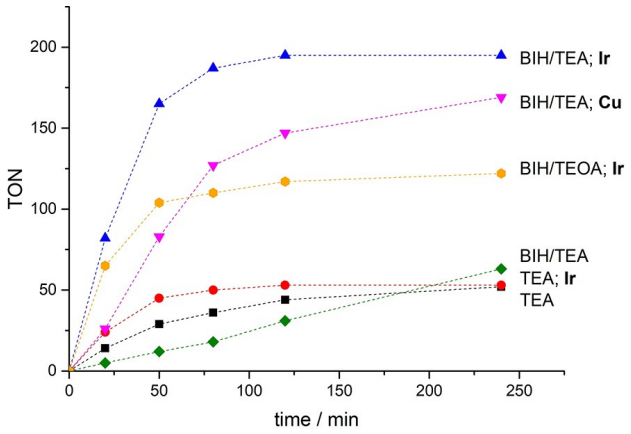

Figure 1. Comparison of catalytic activity of Re_2Cl_2 ($5 \cdot 10^{-5}$ M), in DMF applying a λ > 400 nm longpass filter, different types of SR and a 200 W Xe-lamp. Black: No PS, 5 % (*v/v*) TEA; Green: No PS, 200 eq. BIH/200 eq. TEA; red: 1 eq. **Ir**, 5 % TEA; blue: 1 eq. **Ir**, 200 eq. BIH/200 eq. TEA; orange: 1 eq. **Ir**, 200 eq. BIH/200 eq. TEOA; magenta: 1 eq. **Cu**, 200 eq. BIH/200 eq. TEA.

In addition, the influence of the amount of both, *i.e.* equivalents of photosensitizer and electron donor to catalyst, was investigated (Table 2). While having the highest TON_{CO} using a BIH/TEA combination with both 200 eq., an increase by a factor of 2 of either one or both does not show better catalytic performance. Only an increase by a factor of 5, *i.e.* 1000 eq., leads to a slightly higher CO formation ($TON_{CO,max} = 255$). It is clearly shown that the PS-assisted photocatalysis for Re_2Cl_2 improves the transformation rate of CO_2 to CO. Even low PS equivalents of only 0.1 are able to boost the CO_2 reduction activity. This suggests that the supply of electrons by the light-induced reduced PS is not the limiting factor of catalysis, but rather the subsequent electron (and/or proton) transfer processes.

The results of the photocatalytic experiments seem to suggest that the overspill of reduced PS causes fast catalyst deactivation within the first two hours of catalysis. When using smaller amounts of BIH, *i.e.* 200 eq., almost all electron equivalents end up in the product (CO). Increasing the amount of BIH does not lead to a linear increase of product formation, suggesting that the rhenium catalyst is deactivated before the excess of electron equivalents could be used.

In an additional experiment, we added another 200 eq. each of BIH/TEA after the catalytic activity has ceased for a reaction of Re_2Cl_2 with 1 eq. **Ir** and initially 200 eq. each of BIH/TEA. Surprisingly, no further formation of CO was observed, which suggests again catalyst deactivation. Please note that if a catalytically active form of Re_2Cl_2 would still be present, but **Ir** is decomposed, we should still see a turnover (c.f. green trace in Figure 1).

2.2. Mechanistic Studies

Initial studies by us revealed that the accumulation of two electrons on Re_2Cl_2 by means of photoinduced electron transfer reactions from sacrificial electron donors is hampered by a strong electronic communication between the two metal fragments.[20] However, if the system was reduced twice (*e.g.* by

means of electrochemical reduction), a cooperative behavior was observed as evidenced by a considerably lowered onset potential for electrocatalysis. Furthermore, the reduction of both bpyRe-fragments led to the fast formation of a species with an intramolecular Re–Re bond (*i.e.* **[ReRe]**) that has a more positive reduction potential compared to $[Re(bpy)(CO)_3]_2$. Reductive bond cleavage within this intermediate can therefore be exploited to access up to 4-fold reduced species, as has been evidenced by (spectro-)electrochemical studies.[20]

In order to investigate the reason for the observed catalytic results presented above, mechanistic studies focusing on the electron transfer pathways after light excitation were performed. The addition of an external photosensitizer certainly complicates mechanistic studies and adds complexity to the investigations because multiple reaction pathways are conceivable (Scheme 2). Within this intermolecular three-component system consisting of $\mathbf{Re_2Cl_2}$, photosensitizer and sacrificial reductant several photoinduced electron transfer (PET) and electron transfer (ET) processes are possible for producing catalytically active species, resting states or deactivated products. The most important reaction pathways are a) reductive quenching of photoexcited $\mathbf{Re_2Cl_2}$ by SR (TEA or BIH) to $\mathbf{[Re_2Cl_2]^{1-}}$, b) reductive quenching of photoexcited **PS*** by SR to $\mathbf{PS^{1-}}$, c) oxidative quenching of photoexcited **PS*** by $\mathbf{Re_2Cl_2}$ and d) electron transfer from photoreduced $\mathbf{PS^{1-}}$ to $\mathbf{Re_2Cl_2}$ or $\mathbf{[Re_2Cl_2]^{1-}}$ in the dark. Please note that $\mathbf{[Re_2Cl_2]^{2-}}$ tends to rapidly lose chloride ions to form a Re–Re bond in **[ReRe]** as shown in pathway d. Therefore, the feasibility of the fundamental PET processes between $\mathbf{Re_2Cl_2}$, **Ir**, **Cu** and sacrificial electron donors BIH and TEA (processes a)-c) in Scheme 2) is first elaborated.

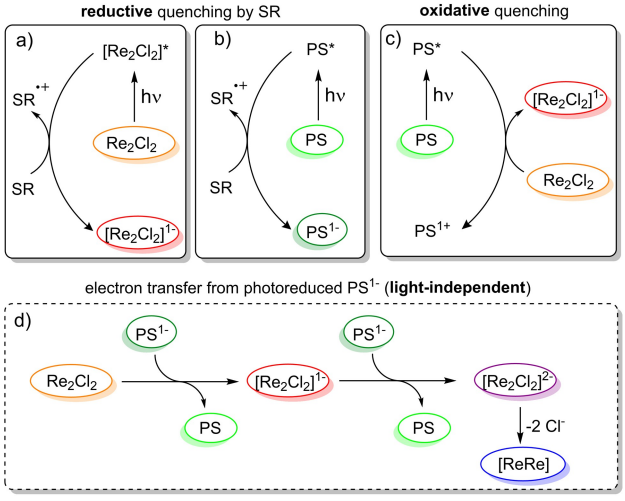

Scheme 2. Possible electron transfer reactions between $\mathbf{Re_2Cl_2}$, PS and SR for the formation of doubly-reduced $\mathbf{[Re_2Cl_2]^{2-}}$ by photochemically produced reducing agent $\mathbf{PS^{1-}}$. Reactions in solid boxes are light-induced reactions, whereas reactions in dashed box are light-independent (for calculated reaction energies see Table S1).

2.3. Reductive Quenching of Re_2Cl_2 (Scheme 2a)

The efficient nature of reductive quenching of excited ^{3}MLCT states of Re^{I} tricarbonyl complexes has already been studied extensively.[52–55] In line with these findings, the bimolecular quenching constant for $\mathbf{Re_2Cl_2}$ obtained from Stern-Volmer analysis is $k_q = 1.4 \cdot 10^{10}\ M^{-1}s^{-1}$ for BIH[20] and $k_q = 2.52 \cdot 10^{8}\ M^{-1}s^{-1}$ for TEA in DMF (Figure S1). The higher rate constant for quenching with BIH is clearly attributed to the lower oxidation potential of BIH compared to TEA (Table 1).[53] In both cases reductive quenching is occurring efficiently, and reduced species can accumulate during continuous irradiation.

2.4. Reductive quenching of PS (Scheme 2b)

It is also known that **Cu** can undergo reductive quenching with TEA and BIH, the quenching rate constant is $k_q = 2.9 \cdot 10^{9}\ M^{-1}s^{-1}$ for BIH (in DMA/TEOA (4:1 *v/v*, DMA = *N*,*N*-dimethylacetamide) with $\tau_0 = 240$ ns).[37,56] Quenching of **Ir** by BIH has been confirmed by Stern-Volmer analysis, with $k_q = 2.62 \cdot 10^{9}\ M^{-1}s^{-1}$ (Figure S1). Due to the high oxidative power of the ^{3}MLCT state of **Ir** (Table 1) a fast formation of $\mathbf{Ir^{1-}}$ can be assumed. Notably, reductive quenching of **Ir** with TEA should be energetically disfavored, due to the higher oxidation potential of TEA in DMF (Table 1). This assumption is indeed in line with catalytic results, as the combination of **Ir** and just 5% TEA in DMF shows no improvement in catalysis (Table 2, entry 1).

2.5. Oxidative quenching of PS by Re_2Cl_2 (Scheme 2c)

Further, we also investigated the oxidative quenching pathway of the photosensitizers (Scheme 2, process c) with $\mathbf{Re_2Cl_2}$ by means of Stern-Volmer analysis. Clear evidence for electron or energy transfer is given by a decrease in ^{3}MLCT lifetimes of **Ir** (10 μM) and **Cu** (50 μM) from 1559 ns to 1195 ns and 297 ns to 245 ns, at 100 and 500 μM $\mathbf{Re_2Cl_2}$, respectively (Figure S2 and S3). Please note that quenching studies with **Cu** were performed in acetonitrile, since the emission in DMF is very weak, and therefore, the emission of $\mathbf{Re_2Cl_2}$ ($\lambda_{em} = 597$ nm) is superimposing even at very low concentrations. Interestingly, the Stern-Volmer analysis of **Ir** displays not only collisional, but also static quenching behavior (Figure S2). Furthermore, oxidative quenching with **Cu** is around two orders of magnitude more efficient than it is for **Ir** (Table S2).[57,58]

Time-dependent UV/vis measurements during continuous irradiation (with $\lambda > 360$ nm) of a 1:1 mixture of $\mathbf{Re_2Cl_2}$ and **Ir** (50 μM) in DMF in the absence of an electron donor confirmed the oxidative nature of this quenching process (*i.e.* Scheme 2c) by formation of $\mathbf{[Re_2Cl_2]^{1-}}$ with characteristic signals at 450 and 580 nm (Figure S2).[20] The cage escape yield, which reflects the efficiency with which the redox reaction products are separated into bulk solution after electron-transfer,[59] is $\Phi = 0.12$. The value was determined with the attenuation coefficient ($\varepsilon_{580\ nm} = 4.36 \cdot 10^{3}\ M^{-1}cm^{-1}$, SI page 8) of $\mathbf{[Re_2Cl_2]^{1-}}$ and is in the same order as is typically observed for the oxidative quenching of

Ru^{II} and Os^{II} metal complexes,[59,60] but lower than for reductive quenching processes of Re^{I} complexes.[61] However, the reductive quenching efficiency of the single collisions ($\eta_q = [Q] \times K_{SV}/(1 + [Q] \times K_{SV})$, Q=Quencher, K_{SV} values are listed in Table S2) of **Ir** and **Cu** using BIH at catalysis concentrations ([BIH] = 10 mM (*i.e.* 200 eq.), Table 2) $\eta_q > 97\%$ and 87% is very effective. In contrast, under oxidative conditions using $\mathbf{Re_2Cl_2}$ (c = 50 μM), the values obtained are very low ($\eta_q < 0.2\%$ (**Ir**) and < 3% (**Cu**)), which means that this process can be neglected under catalytic conditions (Scheme 2c).[37]

2.6. Electron transfer from photoreduced PS^{1-} to $[Re_2Cl_2]^{1-}$

After having evaluated the likelihood of fundamental reaction pathways (in particular Scheme 2a and b), which are a prerequisite for the formation of higher reduced states, like $[\mathbf{Re_2Cl_2}]^{2-}$, *via* PS-assisted reduction, our attention turned to possible implications on chemical reactivity (Scheme 2d). On account of the close vicinity of the two metal centers, $\mathbf{Re_2Cl_2}$ tends to form a Re–Re bond when both bpyRe-units are reduced once, *i.e.* formation of $[\mathbf{Re_2Cl_2}]^{2-}$ induces rapid chloride loss and transformation to **[ReRe]** (Scheme 2d).[20] This species is considered to be a possible resting state during catalysis and does not present a deactivation product.[19] **[ReRe]** has a pronounced and characteristic band at 810 nm in the UV/vis spectrum, which is persistent against oxidative conditions such as potentials more negative than $[\mathbf{ReRe}]^{+/0} = -0.46$ V *vs.* Fc/Fc^+ (Figure S4) or air (at least on a short time scale). Since this band is also well separated from any other absorption features of one of the two photosensitizers ($\varepsilon_{\lambda > 500\ nm} \approx 0$ for **Cu** and **Ir**),[49,50] it can therefore be used to verify the success of a two-electron reduction process.

However, the formation of **[ReRe]** (or formally $[\mathbf{Re_2Cl_2}]^{2-}$) is only possible if photoreduced $\mathbf{PS}^{1-}$ is able to transfer an electron to $[\mathbf{Re_2Cl_2}]^{1-}$ (Scheme 2d). This process is addressed by transient absorption spectroscopy: When exciting a mixed solution containing $\mathbf{Re_2Cl_2}$, **Ir** (0.1 mM each) and BIH (5 mM) at 355 nm, addressing MLCT states of both complexes, a new long-lived (≫ 5 μs) signal at 810 nm can be recorded (Figure S5). Without photosensitizer, $\mathbf{Re_2Cl_2}$ has an excited state absorption spectrum similar to mononuclear **bpy-Re** and exhibits no such signal (Figure S6).[52,62,63] Since none of the complexes has (excited state) absorption features in this wavelength range, the signal can (tentatively) be assigned to **[ReRe]**. Additionally, the kinetic profile of the signal recorded at 560 nm is slightly changed upon addition of **Ir** (compare Figure S7 and S5). The intensity of the signal keeps increasing even after a first rise which is indicative of follow-up reactions such as for example electron transfer reactions from $\mathbf{Ir}^{1-}$. The same behavior is also observed in the case when **Cu** is used as photosensitizer (Figure S8). Interestingly, this second process takes place in the same time regime (*i.e.* < 300 ns), as the formation of the long-lived signal at 810 nm (Figure S5).

For both photosensitizers, **Ir** and **Cu**, the formation of **[ReRe]** can also be verified by time-dependent UV/vis measurements during irradiation (hν > 360 nm) of a solution containing $\mathbf{Re_2Cl_2}$ and PS in equimolar amounts (0.05 mM) in the presence of BIH/TEA (5/10 mM) and subsequent aeration of the reaction mixture (Figure S9). The last step is mandatory, since formation of **[ReRe]** is not selective and other reaction products such as singly-reduced $[\mathbf{Re_2Cl_2}]^{1-}$ are superimposing the absorption spectrum.[20] However, the reduction process of singly reduced species is fully reversible and UV/vis signals therefore vanish completely under air without the formation of side-products. Hence, only the new signals of **[ReRe]** remain after aeration. The same reactivity is also observed with significantly reduced amounts of SR (10 eq. BIH, Figure 2), which indicates a high efficiency of the quenching of the respective ^{3}MLCT states as well as the efficacy of the electron transfer process from $\mathbf{PS}^{1-}$ to $[\mathbf{Re_2Cl_2}]^{1-}$ (*vide infra*).

Furthermore, the formation of **[ReRe]** is absent when irradiating with λ > 460 nm, because the PS does not absorb any light in this wavelength range (Figure S12).

The effect of TEA as an additive to BIH to deprotonate $BIH^{\bullet+}$ and to limit unproductive charge recombination was recently described.[48] Surprisingly, when TEA (or TEOA) is used in commonly applied catalytic concentrations (*i.e.* 5% or 20%, *v/v* respectively)[44,64] the signal at 810 nm is not formed and only $[\mathbf{Re_2Cl_2}]^{1-}$ is accumulated (Figure S10 and S13). However, the necessity of TEA is more pronounced for **Cu** and no Re–Re bond formation can be seen if only BIH is used in this case (Figure S11). In addition, widely used triethanolamine (TEOA, 20% *v/v*) seems to be detrimental for the accumulation of [ReRe] (d in Scheme 2), since i) slow deprotonation of $BIH^{\bullet+}$ may be insufficient to kinetically compete with charge recombination from the reductively quenched species to oxidized $BIH^{\bullet+}$

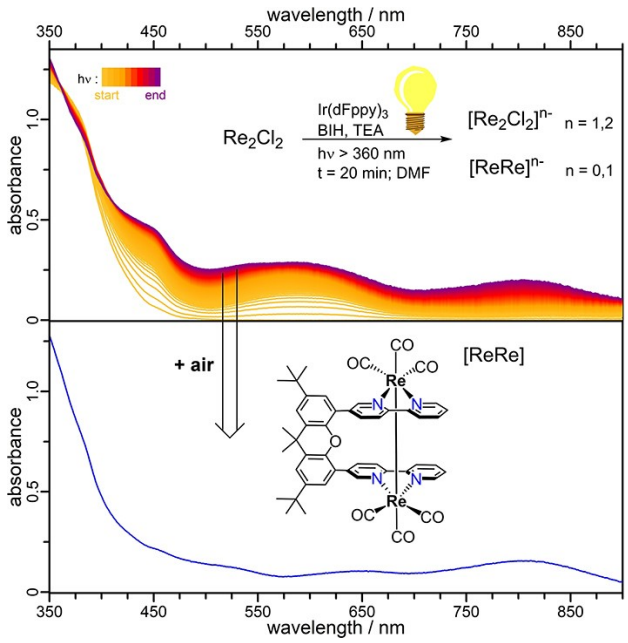

Figure 2. Top: Time-dependent UV/Vis absorption spectroscopic measurements of $\mathbf{Re_2Cl_2}$ (50 μM) in DMF with **Ir**/BIH/TEA (1/10/20 eq.) during continuous irradiation (orange to dark magenta). Bottom: UV/Vis spectrum of **[ReRe]** (blue) obtained by aeration of the solution after 20 min of illumination.

[48] and ii) formation of Re-TEOA adducts may compete with Re–Re bond formation.[47,65] The spectroscopic results confirm the catalytic observations described above, in which the combination of BIH/TEA gives highest turnover numbers. This is surprising, since the possibility of Re–Re bond formation obviously exceeds the beneficial effect of CO_2-capture by TEOA-adducts.[47]

As a collision induced process, the light-independent reduction process/electron transfer from $\mathbf{PS}^{1-}$ to $[\mathbf{Re_2Cl_2}]^{1-}$ (Scheme 2d) is dependent on the diffusion ability, concentration, and the lifetime of the intermediates. Exemplarily for this photosensitized mechanism the concentration dependence of **Ir** and BIH has been investigated. For this purpose, the evolution of the absorbances at 580 nm and 810 nm were evaluated, because these signals are characteristic for the formation of $[\mathbf{Re_2Cl_2}]^{1-}$ and **[ReRe]**, respectively (Table 1). When irradiating $\mathbf{Re_2Cl_2}$ and **Ir** (50 μM each) in the presence of BIH (50 μM) fast formation of signals at 450, 580 and 810 nm are observed (Figure S14). The accumulation of **[ReRe]** starts at a BIH concentration of 50 μM (1 eq.). A further increase in the concentration of BIH does not change the initial process, the band shape or the band positions. In general, the light-induced process can be characterized by three distinctive time intervals: fast increase of absorbance (1st phase), succeeded by a follow-up reaction (see "bump" at ~45 s in the absorbance at 580 nm, 2nd phase) and further a slight increase in intensity (3rd phase, Figure S14). Overall, there is a pronounced concentration dependency on the evolution of the signal at 810 nm, which reaches its peak at $c_{BIH} = 1.25$ mM (*i.e.* 25 equivalents w.r.t. $\mathbf{Re_2Cl_2}$, $A_{810\ nm} = 0.21$) and decreases again at higher concentrations of BIH.

On the other hand, if the concentration of BIH is kept constant and the amount of **Ir** is changed, a different, linear correlation is observed (Figure S15). Increasing the amount of **Ir** leads to a faster formation as well as larger intensity of absorbance at 810 nm. Even with PS loadings of only 2.5 μM (0.05 equivalents w.r.t. $\mathbf{Re_2Cl_2}$) an absorption signal is observed at 810 nm. The assignment of this signal to **[ReRe]** was again verified by exchanging the inert atmosphere with air. However, when increasing the amount of **Ir** (*i.e.* 4 eq.) new shoulders at 540 nm and 640 nm are formed (Figure S15). Since there is no substrate at this stage, these new absorption features can only belong to higher reduced states of $\mathbf{Re_2Cl_2}$. Indeed, such signals are also observed for $\mathbf{Re_2Cl_2}$ in DMF under spectroelectrochemical conditions for applied potentials of $-1.81 < E < -1.96$ V.[20] At these potentials it is expected that $[\mathbf{Re_2Cl_2}]^{2-}$ and $[\mathbf{ReRe}]^{1-}$ will be formed (see also Figure S4). However, it is questionable whether these new bands develop as a result of consecutive electron transfer processes or due to photoinduced reactions of accumulated reaction intermediates. Hence, the photoinduced cleavage of Re–Re bonded species can be a feasible reaction pathway due to the lower stability of the Re–Re bond in the xanthene bridged dinuclear complex.[20]

For further analysis, the light-induced formation of reducing equivalents (*i.e.* $\mathbf{Ir}^{1-}$) was separated from the electron transfer process(es) by experimental design (see Scheme S2 and Figure S16). Adding a solution of photo reduced $\mathbf{Ir}^{1-}$ (50 nmol) to a solution of $\mathbf{Re_2Cl_2}$ (100 nmol in DMF) only leads to the formation of a signal at 580 nm. At a higher amount of $\mathbf{Ir}^{1-}$ (100—200 nmol) there is a subsequent formation of an absorption band at 810 nm as a result of a slow electron transfer from $\mathbf{Ir}^{1-}$ to $[\mathbf{Re_2Cl_2}]^{1-}$. Interestingly, the formation of **[ReRe]** is initiated with a 1:1 stoichiometry of photoreduced **Ir** to dinuclear $\mathbf{Re_2Cl_2}$. Additionally, at a higher concentration the band shape changes around 580 nm and new signals (shoulders) are formed at 640 and 720 nm (Figure S16). These signals are indicative for the formation of higher reduced species with formally two-fold reduced bpyRe-units, such as $[\mathbf{Re_2}]^{1-}$ and $[\mathbf{Re_2}]^{2-}$, as very similar spectra are obtained in UV/vis spectroelectrochemical measurements at applied potentials of $-2.16 < E < -2.36$ V.[20] These species with formal $Re^0(bpy^{\bullet-})$ moieties are considered to be catalytically more potent intermediates than singly-reduced bpyRe-units.[46,66,67]

A plausible explanation for the formation of these higher reduced products is that the reductive quenching of **Ir** by BIH formally produces two redox equivalents under this condition: One redox equivalent is $\mathbf{Ir}^{1-}$ and the other is the $BIH^{\bullet+}$ radical cation, which has a high reductive power after deprotonation ($E^{ox}(BI^{\bullet}) = -2.06$ vs. $Fc^{+/0}$)[68] and participates in an equilibrium with its dimerized product $(BI)_2$.[69] An accumulation of both redox equivalents $\mathbf{Ir}^{1-}$ and $BI(H)^{\bullet(+)}$ is possible due to the efficient reductive quenching process ($k_q = 2.62 \cdot 10^9\ M^{-1}s^{-1}$, Table S2) and because an electron transfer from $BI^{\bullet}$ to **Ir** is thermodynamically not possible. Consequently, the reduction of $[\mathbf{Re_2Cl_2}]^{n-}$ (with n = 0,1), as well as the formation of higher reduced species by the $\mathbf{Ir}^{1-}/BI(H)^{\bullet(+)}$ mixture is possible. The use of a BIH/TEA mixture instead of only BIH to form the reduced PS does not lead to any significant changes (Figure S16), but only increases the overall yield of reduced $\mathbf{Re_2Cl_2}$ reaction products. Most likely the slowed back electron transfer reactions due to the deprotonation of $BIH^{\bullet+}$ by TEA ($k_{dp} = 5.5 \cdot 10^5\ M^{-1}s^{-1}$)[48] are the reason for this observation.

The determination of the amount of **[ReRe]** (as well as $[\mathbf{Re_2Cl_2}]^{1-}$) generated in the photochemical reaction between $\mathbf{Re_2Cl_2}$ and **Ir** in the presence of BIH was then investigated by titration experiments with stochiometric amounts of a Rh^{III} electron acceptor such as [Rh(phen)(Cp*)Cl]Cl (phen = 1,10-phenanthroline, $Cp^* = C_5Me_5$, $E^{II/III} = -1.2$ V, Figure 3 and S17). Monoelectronic reduction of this complex leads to an intermediate formation of a Rh^{II} species which undergoes fast disproportionation to form a stable Rh^{I} species.[70,71] When the Rh^{III} complex is added to a previously irradiated solution (Figure 3, process indicated by grey arrow) containing the photo reduced products, the characteristic signal of $[\mathbf{Re_2Cl_2}]^{1-}$ at 580 nm gradually disappears, while a characteristic and well-separated absorption of reduced Rh^{I} species is formed ($\lambda =$ 680 nm, Figure 3, process marked by blue arrows, and Figure S17). The saturation of the absorption of the Rh^{I} species is reached as soon as all redox equivalents from photoreduced products have been transferred to the initial Rh^{III} species. This condition is fulfilled with $n(Rh^{III}) \geq 50$ nmol for the case that only $\mathbf{Re_2Cl_2}$ (100 nmol) and BIH (5 μmol) were irradiated. This is equivalent to the selective and quantitative formation of $[\mathbf{Re_2Cl_2}]^{1-}$ (Figure 3). On the contrary, if **Ir** (100 nmol) is also

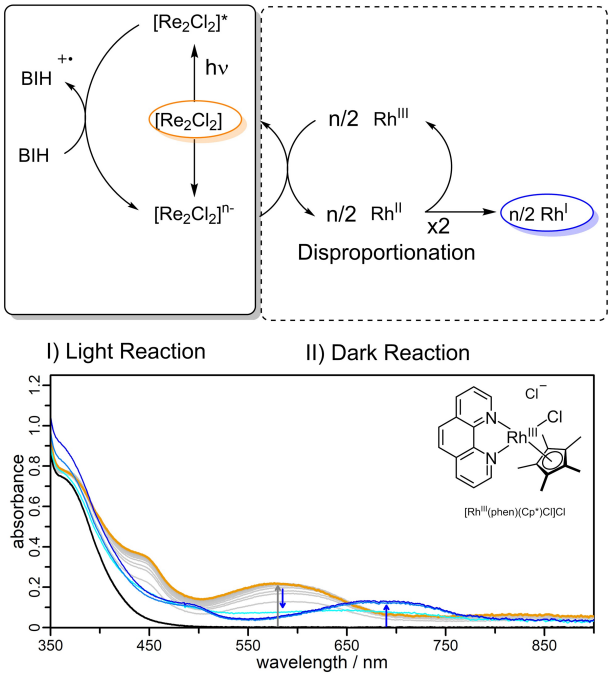

Figure 3. Top: Mechanism of electron transfer from photoreduced $\mathbf{Re_2Cl_2}$ to $[Rh^{III}(phen)(Cp^*)Cl]Cl$. Please note: Due to the disproportionation reaction of the Rh^{II} intermediate, the formation of one molecule of reduced rhodium complex (*i.e.* Rh^{I}) requires two-electrons. **Bottom**: UV/Vis absorption spectrum of $\mathbf{Re_2Cl_2}$ (100 nmol) and BIH (5 µmol) in DMF (2 mL) during irradiation (light- to dark-grey) and after photoreduction ceased (orange). Thereafter, the light source was removed and aliquots of $[Rh^{III}(phen)(Cp^*)Cl]Cl$ (2 mM) with n = 5 nmol (cyan), 50 nmol (blue) and n = 100 nmol (dark blue) were added. The experiments were repeated with new solutions for every concentration of Rh^{III}-complex. After an addition of 50 nmol (0.5 equiv w.r.t. $\mathbf{Re_2Cl_2}$) the reaction reaches a steady state. This implies that in total 1.0 electron per molecule $\mathbf{Re_2Cl_2}$ has been transferred to the rhodium complex.

present, only $n(Rh^{III}) \geq 15$ nmol are required to completely oxidize photoreduced reaction products (Figure S17). It follows, that 0.6 electrons per molecule $\mathbf{Re_2Cl_2}$ are stored in the reaction mixture (*i.e.* oxidation of ≈60 nmol of $[\mathbf{Re_2Cl_2}]^{1-}$) and the ≈40 nmol (40%) of initially converted $\mathbf{Re_2Cl_2}$ remain due to the formation of **[ReRe]**, which cannot interact with the Rh^{III} complex (Figure S17).

However, this concentration ratio is only a snapshot, since the absorbance at 810 nm increases significantly with longer irradiation times (*c.f.* Figure S14–15). Even after 30 minutes of irradiation no quantitative transformation of $[\mathbf{Re_2Cl_2}]^{1-}$ to **[ReRe]** could be achieved regardless of the reaction conditions. Since the electron transfer from $\mathbf{Ir}^{1-}$ to $[\mathbf{Re_2Cl_2}]^{1-}$ is very efficient in the dark (*c.f.* Figure S16), this slow accumulation of **[ReRe]** is most likely attributed to counterproductive light-induced reactions such as the photolysis or photoreduction of the Re–Re bonded species.

2.7. Photoreactivity with CO_2

In a next step the reactivity of photoreduced complexes with CO_2 was investigated by time-dependent UV/vis and IR studies under photocatalytic conditions. Surprisingly, the absorption spectrum obtained for a 1:1 mixture of $\mathbf{Re_2Cl_2}$ with **Ir** (50 µM each) in presence of BIH/TEA under 1 atm CO_2 (Figure 4, top) is markedly different from any reaction described so far: A fast formation of an absorption feature at 580 nm, indicative for $[\mathbf{Re_2Cl_2}]^{1-}$ (Table 1), is observed within the first 40 seconds. Thereafter, simultaneous formation of a signal at 540 nm as well as a broad absorption with an absorbance maximum > 900 nm is observed (Figure 4, phase I, top).

When the light-source is removed (phase II, Figure 4, bottom), the signals at 540, 580 and around 900 nm decrease again. Surprisingly, the spectrum obtained at the end of the dark phase no longer changes after further aeration, but matches quite well to the spectrum of **[ReRe]**. This observation indicates that 1) light is required for the catalytic turnover and 2) formation of Re–Re bonds also occurs under CO_2 saturated conditions. The decay of the absorption feature between 500–600 nm, after the light source is removed, can be analyzed by a mono-exponential function (Figure S18-S20). Half-life's of the reduced species/intermediates are considerably reduced under CO_2 compared to argon atmosphere (Table S4). In addition, faster reaction kinetics in the presence of PS is confirmed – nicely in line with the results of the photocatalytic experiments (*vide supra*).

In a similar experiment with continuous irradiation (no dark phase), the signals at 540 and around 900 nm also decay within 30 min (Figure S21). Contrary to the decay in the dark, however, the signal intensities are strongly diminished and essentially only the absorption band at 580 nm remains. This can be reasoned to the onset of rapid catalytic transformations. The

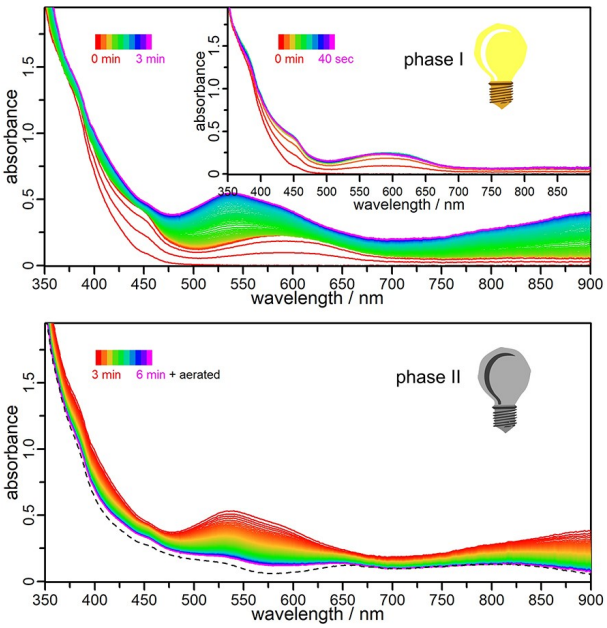

Figure 4. Time-dependent UV/Vis absorption spectrum of $\mathbf{Re_2Cl_2}$ (0.05 mM) with **Ir** (0.05 mM) in $\mathbf{CO_2}$-saturated DMF in the presence of BIH (5 mM) and TEA (10 mM) under $\mathbf{1^{st}}$ irradiation for 3 minutes (phase I, top figure), $\mathbf{2^{nd}}$ subsequent storage in the dark for 3 minutes and $\mathbf{3^{rd}}$ after exposure to air (black dotted line, bottom figure). Irradiation condition: 150 W Xe-arc lamp, λ > 360 nm. A kinetic analysis and determination of decay constants is given in the supporting information (Figure S18).

residual signal at 580 nm can most likely be assigned to $[Re_2Cl_2]^{1-}$ which only slowly interacts with CO_2.[20] A similar reactivity is also observed when **Cu** is used as a photosensitizer (Figure S21). In this case, however, the depletion of absorption is less pronounced, which can be correlated with the somewhat lower formation rate of CO in the catalytic experiments (Figure 1, Table 2). The new signal at 540 nm can presumably be assigned to either $[ReRe]^{1-}$ (*vide supra*) or a CO_2-adduct (*vide infra*, Figure S22), while absorption > 900 nm is quite unusual. The latter absorption feature is not observed in the absence of PS (Figure S19) and only observed under CO_2 atmosphere and might tentatively be assigned to a (reduced) CO_2 adduct in which both rhenium center coordinate to the CO_2 molecule (see further discussion below).

The process of photocatalytic conversion was further monitored by IR spectroscopy (Figure S22). The stoichiometry between Re_2Cl_2/**Ir**/BIH was kept constant, but the concentration had to be increased by a factor of 20, which could potentially initiate different reaction pathways. During the first two minutes of irradiation, characteristic signals of $[Re_2Cl_2]^{1-}$ (1995, 1882, 1866 cm^{-1}) and **[ReRe]** (1981, 1946, 1848 cm^{-1}) as well as additional signals of a new intermediate at 2003 and 1990 cm^{-1} were formed (Figure S22, Table S5). Furthermore, overlapping signals at 1898 and 1866 cm^{-1} can be identified by comparison to IR experiments under argon atmosphere in the absence of **Ir**.[20] These signals can be assigned to a CO_2-bridged species **[Re(μ-CO$_2$)Re]** (Scheme S3), because of the well matching signals of $[Re(bpy)(CO)_3](CO_2)$ at 2002, 1989, 1896 and 1867 cm^{-1} (Table S6).[72] The IR data therefore suggest that addition of CO_2 competes with the Re–Re bond formation and that the activation of CO_2 occurs through bimetallic activation by two singly-reduced bpyRe-units. Further irradiation (5–10 min) leads to the decline of signals of **[ReRe]**, indicating that the Re–Re bond is cleaved during photocatalysis.[19] At later times (20–30 min) the signals at 2003, 1990, 1898 and 1866 cm^{-1} are also depleting and a new signal with a maximum at 2014 cm^{-1} is formed. However, the parent signal of Re_2Cl_2 at 2022 cm^{-1} is clearly affected and eventually masking the true band position or further signals. Additionally, another signal around ~1917 cm^{-1} is evolved, but is overlapped with the bleach of Re_2Cl_2 at 1919 cm^{-1}.[20] The high frequency vibration mode $\nu(CO) = 2014$ cm^{-1} of this new species (Table S5) indicates an oxygen-coordination to the rhenium center, as has been found in carbonate-bridged $[Re(dmbpy)(CO)_3]_2(OCO_2)$ (2011, 1899, 1867 cm^{-1}) or carboxylate coordinated Re(dmbpy)$(CO)_3$(OC(O)OH) (2017, 1912, 1888 cm^{-1}, Table S6).[72] Both species have been identified as oxidation products during the photolysis of $[Re(dmbpy)(CO)_3]_2(CO_2)$, and hence, similar reactions are expected for **[Re(μ-CO$_2$)Re]** (Scheme S3).[72]

3. Conclusion

Cooperative bimetallic activation of CO_2 can be of great advantage compared to monometallic-single site activation, because electron transfer reactions can be efficiently channeled. The dinuclear Re^{I} complex Re_2Cl_2 has previously demonstrated an increased photocatalytic activity (up to 45-fold higher TON_{CO}) compared to monometallic $[Re(bpy)(CO)_3Cl]$, although bimetallic activation by two singly-reduced bpyRe-units could not be proven explicitly. Therefore, external photosensitizers with suited redox potentials and excited state energies were used in this study to a) elucidate the mechanisms of electron transfer to Re_2Cl_2 *via* light-driven generation of strong reductants b) enable bimetallic activation of CO_2. As a result, a strong enhancement of photocatalytic CO_2 to CO reduction by the addition of the external photosensitizers to the dinuclear rhenium complex could be demonstrated. An Ir^{III} as well as a Cu^{I} photosensitizer were able to increase the catalytic turnover by a factor of at least 4. The efficiency of the electron transfer and thus the turnover frequency is higher for **Ir**. Surprisingly, the usually observed longevity of the rhenium-based catalysts is not seen in the presence of an added PS and catalysis stops after about two hours, while it still continuous after 24 hours of illumination without PS.

Mechanistic investigations using nanosecond transient absorption and time-dependent UV/vis spectroscopy confirmed for the first time that the interaction of a reduced photosensitizer with Re_2Cl_2 generates an intermediate with two singly reduced bpyRe-units. If a solution of Re_2Cl_2 and BIH without PS is irradiated, the selective and quantitative formation of mono-reduced species $[Re_2Cl_2]^{1-}$ can be observed. However, if **Ir** is used as PS, the electron transfer from Ir^{1-} to $[Re_2Cl_2]^{1-}$ is very efficient and enables the accumulation of double reduced species, such as intermediate **[ReRe]** possessing a Re–Re bond. No quantitative formation of **[ReRe]** is observed, most likely due to light-induced follow-up reactions such as the photolysis of the Re–Re bond and creation of higher-reduced species. Interestingly, within this intermolecular arrangement an efficient electron transfer from the photosensitizer to the catalyst occurs, even when the PS is applied in very low amounts as low as 0.05 equivalents. IR spectroscopy under photocatalytic conditions clearly revealed the formation of a CO_2-bridged intermediate, and hence bimetallic activation of CO_2 was proven.

In summary, we obtained new insights on the reaction mechanism of bimetallic CO_2 activation. The key steps are i) efficient and fast build-up of redox equivalents PS^{1-} (PS=Ir^{III} or Cu^{I} photosensitizer); ii) efficient electron transfer from PS^{1-} to $[Re_2Cl_2]^{n-}$ (n = 0,1) and formation of higher reduced species such as $[Re_2Cl_2]^{2-}$ and **[ReRe]**; iii) bimetallic activation of CO_2 and formation of **[Re(μ-CO$_2$)Re]**. In this scenario the supply of electrons *via* the photoreduced PS is not the limiting factor for catalytic transformation, but rather the subsequent electron (and/or proton) transfer processes. The results demonstrate that thermodynamic constraints can be overcome by carefully revising the catalytic system. Further investigations will focus on determining the crucial intermediates after CO_2 activation.

Experimental Section

Supplementary data associated with this article as well as general information on the experimental details (photocatalysis, NMR, IR,

UV/vis and nanosecond time-resolved spectroscopy, UV/vis spectroelectrochemistry) can be found in the supporting information (SI).

Acknowledgements

Financial support from the German Research Foundation (Deutsche Forschungsgemeinschaft, DFG, TS330/3-1 for ST) is highly appreciated. MS thanks UniSysCat funded by the DFG under Germany's Excellence Strategy – EXC 2008/1-390540038-UniSysCat. We are further thankful to the priority program 2102 Light-controlled reactivity of metal complexes (DFG SCHW1454/9-1, KA 4671/2-1 and TS330/4-1). We also thank Alexander Mengele for his support with the Rh complex. Open access funding enabled and organized by Projekt DEAL.

Conflict of Interest

The authors declare no conflict of interest.

Keywords: bimetallic activation · carbon dioxide reduction · cooperative effects · photocatalysis · rhenium

[1] T. Ouyang, H.-J. Wang, H.-H. Huang, J.-W. Wang, S. Guo, W.-J. Liu, D.-C. Zhong, T.-B. Lu, *Angew. Chem. Int. Ed.* **2018**, *57*, 16480–16485.
[2] A. W. Nichols, C. W. Machan, *Front. Chem.* **2019**, *7*, 397.
[3] Z. Guo, G. Chen, C. Cometto, B. Ma, H. Zhao, T. Groizard, L. Chen, H. Fan, W.-L. Man, S.-M. Yiu, K.-C. Lau, T.-C. Lau, M. Robert, *Nat. Can.* **2019**, *2*, 801–808.
[4] Y. Pellegrin, F. Odobel, *Coord. Chem. Rev.* **2011**, *255*, 2578–2593.
[5] A. M. Appel, J. E. Bercaw, A. B. Bocarsly, H. Dobbek, D. L. DuBois, M. Dupuis, J. G. Ferry, E. Fujita, R. Hille, P. J. A. Kenis, C. A. Kerfeld, R. H. Morris, C. H. F. Peden, A. R. Portis, S. W. Ragsdale, T. B. Rauchfuss, J. N. H. Reek, L. C. Seefeldt, R. K. Thauer, G. L. Waldrop, *Chem. Rev.* **2013**, *113*, 6621–6658.
[6] L. Hammarström, *Acc. Chem. Res.* **2015**, *48*, 840–850.
[7] A. Pannwitz, O. S. Wenger, *Chem. Commun.* **2019**, *55*, 4004–4014.
[8] A. F. Heyduk, D. G. Nocera, *Science* **2001**, *293*, 1639–1641.
[9] R. Konduri, H. Ye, F. M. MacDonnell, S. Serroni, S. Campagna, K. Rajeshwar, *Angew. Chem. Int. Ed.* **2002**, *41*, 3185–3187; *Angew. Chem.* **2002**, *114*, 3317–3319.
[10] R. Konduri, N. R. de Tacconi, K. Rajeshwar, F. M. MacDonnell, *J. Am. Chem. Soc.* **2004**, *126*, 11621–11629.
[11] Y. Na, P. Lincoln, J. R. Johansson, B. Nordén, *ChemCatChem* **2012**, *4*, 1746–1750.
[12] K. Kitamoto, K. Sakai, *Chem. Commun.* **2016**, *52*, 1385–1388.
[13] J.-F. Lefebvre, J. Schindler, P. Traber, Y. Zhang, S. Kupfer, S. Gräfe, I. Baussanne, M. Demeunynck, J.-M. Mouesca, S. Gambarelli, V. Artero, B. Dietzek, M. Chavarot-Kerlidou, *Chem. Sci.* **2018**, *9*, 4152–4159.
[14] M. Schulz, N. Hagmeyer, F. Wehmeyer, G. Lowe, M. Rosenkranz, B. Seidler, A. Popov, C. Streb, J. G. Vos, B. Dietzek, *J. Am. Chem. Soc.* **2020**, *142*, 15722–15728.
[15] T. J. Whittemore, C. Xue, J. Huang, J. C. Gallucci, C. Turro, *Nat. Chem.* **2020**, *12*, 180–185.
[16] X. Zhang, M. Cibian, A. Call, K. Yamauchi, K. Sakai, *ACS Catal.* **2019**, *9*, 11263–11273.
[17] W. Yang, S. Sinha Roy, W. C. Pitts, R. L. Nelson, F. R. Fronczek, J. W. Jurss, *Inorg. Chem.* **2018**, *57*, 9564–9575.
[18] N. P. Liyanage, W. Yang, S. Guertin, S. Sinha Roy, C. A. Carpenter, R. E. Adams, R. H. Schmehl, J. H. Delcamp, J. W. Jurss, *Chem. Commun.* **2019**, *55*, 993–996.
[19] P. Lang, R. Giereth, S. Tschierlei, M. Schwalbe, *Chem. Commun.* **2019**, *55*, 600–603.
[20] R. Giereth, P. Lang, E. McQueen, X. Meißsner, B. Braun-Cula, C. Marchfelder, M. Obermeier, M. Schwalbe, S. Tschierlei, *ACS Catal.* **2021**, *11*, 390–403.
[21] B. Gholamkhass, H. Mametsuka, K. Koike, T. Tanabe, M. Furue, O. Ishitani, *Inorg. Chem.* **2005**, *44*, 2326–2336.
[22] S. Sato, K. Koike, H. Inoue, O. Ishitani, *Photochem. Photobiol. Sci.* **2007**, *6*, 454–461.
[23] T. L. Easun, W. Z. Alsindi, M. Towrie, K. L. Ronayne, X.-Z. Sun, M. D. Ward, M. W. George, *Inorg. Chem.* **2008**, *47*, 5071–5078.
[24] Z.-Y. Bian, S.-M. Chi, L. Li, W. Fu, *Dalton Trans.* **2010**, *39*, 7884–7887.
[25] Y. Tamaki, K. Watanabe, K. Koike, H. Inoue, T. Morimoto, O. Ishitani, *Faraday Discuss.* **2012**, *155*, 115–127.
[26] Y. Yamazaki, H. Takeda, O. Ishitani, *J. Photochem. Photobiol. C* **2015**, *25*, 106–137.
[27] S. Meister, R. O. Reithmeier, A. Ogrodnik, B. Rieger, *ChemCatChem* **2015**, *7*, 3562–3569.
[28] Y. Tamaki, O. Ishitani, *ACS Catal.* **2017**, *7*, 3394–3409.
[29] L. Frayne, N. Das, A. Paul, S. Amirjalayer, W. J. Buma, S. Woutersen, C. Long, J. G. Vos, M. T. Pryce, *ChemPhotoChem* **2018**, *2*, 323–331.
[30] P. Gotico, A. Del Vecchio, D. Audisio, A. Quaranta, Z. Halime, W. Leibl, A. Aukauloo, *ChemPhotoChem* **2018**, *2*, 715–719.
[31] Y. Tamaki, K. Koike, T. Morimoto, O. Ishitani, *J. Catal.* **2013**, *304*, 22–28.
[32] M. Furue, M. Naiki, Y. Kanematsu, T. Kushida, M. Kamachi, *Coord. Chem. Rev.* **1991**, *111*, 221–226.
[33] K. Koike, D. C. Grills, Y. Tamaki, E. Fujita, K. Okubo, Y. Yamazaki, M. Saigo, T. Mukuta, K. Onda, O. Ishitani, *Chem. Sci.* **2018**, *9*, 2961–2974.
[34] Y. Kuramochi, O. Ishitani, *Inorg. Chem.* **2016**, *55*, 5702–5709.
[35] A. Rosas-Herández, C. Steinlechner, H. Junge, M. Beller, *Green Chem.* **2017**, *19*, 2356–2360.
[36] H. Takeda, H. Kamiyama, K. Okamoto, M. Irimajiri, T. Mizutani, K. Koike, A. Sekine, O. Ishitani, *J. Am. Chem. Soc.* **2018**, *140*, 17241–17254.
[37] Y. Yamazaki, T. Onoda, J. Ishikawa, S. Furukawa, C. Tanaka, T. Utsugi, T. Tsubomura, *Front. Chem.* **2019**, *7*, 288.
[38] A. Call, M. Cibian, K. Yamamoto, T. Nakazono, K. Yamauchi, K. Sakai, *ACS Catal.* **2019**, *9*, 4867–4874.
[39] C. Steinlechner, A. F. Roesel, E. Oberem, A. Päpcke, N. Rockstroh, F. Gloaguen, S. Lochbrunner, R. Ludwig, A. Spannenberg, H. Junge, R. Francke, M. Beller, *ACS Catal.* **2019**, *9*, 2091–2100.
[40] M. Marx, A. Mele, A. Spannenberg, C. Steinlechner, H. Junge, P. Schollhammer, M. Beller, *ChemCatChem* **2020**, *12*, 1603–1608.
[41] T. Koike, M. Akita, *Inorg. Chem. Front.* **2014**, *1*, 562–576.
[42] Y. Zhang, M. Schulz, M. Wächtler, M. Karnahl, B. Dietzek, *Coord. Chem. Rev.* **2018**, *356*, 127–146.
[43] S. Lee, W.-S. Han, *Inorg. Chem. Front.* **2020**, *7*, 2396–2422.
[44] Y. Pellegrin, F. Odobel, *C. R. Chim.* **2017**, *20*, 283–295.
[45] H. Hori, F. P. Johnson, K. Koike, O. Ishitani, T. Ibusuki, *J. Photochem. Photobiol. A* **1996**, *96*, 171–174.
[46] H. Takeda, K. Koike, H. Inoue, O. Ishitani, *J. Am. Chem. Soc.* **2008**, *130*, 2023–2031.
[47] T. Morimoto, T. Nakajima, S. Sawa, R. Nakanishi, D. Imori, O. Ishitani, *J. Am. Chem. Soc.* **2013**, *135*, 16825–16828.
[48] R. N. Sampaio, D. C. Grills, D. E. Polyansky, D. J. Szalda, E. Fujita, *J. Am. Chem. Soc.* **2020**, *142*, 2413–2428.
[49] E. Mejia, S.-P. Luo, M. Karnahl, A. Friedrich, S. Tschierlei, A.-E. Surkus, H. Junge, S. Gladiali, S. Lochbrunner, M. Beller, *Chem. Eur. J.* **2013**, *19*, 15972–15978.
[50] A. B. Tamayo, B. D. Alleyne, P. I. Djurovich, S. Lamansky, I. Tsyba, N. N. Ho, R. Bau, M. E. Thompson, *J. Am. Chem. Soc.* **2003**, *125*, 7377–7387.
[51] A.-M. Manke, K. Geisel, A. Fetzer, P. Kurz, *Phys. Chem. Chem. Phys.* **2014**, *16*, 12029–12042.
[52] K. Kalyanasundaram, *J. Chem. Soc. Faraday Trans. 2* **1986**, *82*, 2401.
[53] J. C. Luong, L. Nadjo, M. S. Wrighton, *J. Am. Chem. Soc.* **1978**, *100*, 5790–5795.
[54] O. Ishitani, M. W. George, T. Ibusuki, F. P. A. Johnson, K. Koike, K. Nozaki, C. Pac, J. J. Turner, J. R. Westwell, *Inorg. Chem.* **1994**, *33*, 4712–4717.
[55] H. Takeda, O. Ishitani, *Coord. Chem. Rev.* **2010**, *254*, 346–354.
[56] S. Fischer, D. Hollmann, S. Tschierlei, M. Karnahl, N. Rockstroh, E. Barsch, P. Schwarzbach, S.-P. Luo, H. Junge, M. Beller, S. Lochbrunner, R. Ludwig, A. Brückner, *ACS Catal.* **2014**, *4*, 1845–1849.
[57] K. L. Cunningham, C. R. Hecker, D. R. McMillin, *Inorg. Chim. Acta* **1996**, *242*, 143–147.
[58] J. Windisch, M. Orazietti, P. Hamm, R. Alberto, B. Probst, *ChemSusChem* **2016**, *9*, 1719–1726.
[59] M. Georgopoulos, M. Z. Hoffman, *J. Phys. Chem.* **1991**, *95*, 7717–7721.
[60] J. Olmsted, T. J. Meyer, *J. Phys. Chem.* **1987**, *91*, 1649–1655.

[61] L. A. Lucia, K. S. Schanze, *Inorg. Chim. Acta* **1994**, *225*, 41–49.
[62] A. El Nahhas, A. Cannizzo, F. van Mourik, A. M. Blanco-Rodríguez, S. Zális, A. Vlček, M. Chergui, *J. Phys. Chem. A* **2010**, *114*, 6361–6369.
[63] S. Sato, Y. Matubara, K. Koike, M. Falkenström, T. Katayama, Y. Ishibashi, H. Miyasaka, S. Taniguchi, H. Chosrowjan, N. Mataga, N. Fukazawa, S. Koshihara, K. Onda, O. Ishitani, *Chem. Eur. J.* **2012**, *18*, 15722–15734.
[64] C. Matlachowski, B. Braun, S. Tschierlei, M. Schwalbe, *Inorg. Chem.* **2015**, *54*, 10351–10360.
[65] H. Kumagai, T. Nishikawa, H. Koizumi, T. Yatsu, G. Sahara, Y. Yamazaki, Y. Tamaki, O. Ishitani, *Chem. Sci.* **2019**, *10*, 1597–1606.
[66] E. E. Benson, C. P. Kubiak, *Chem. Commun.* **2012**, *48*, 7374–7376.
[67] C. W. Machan, S. A. Chabolla, J. Yin, M. K. Gilson, F. A. Tezcan, C. P. Kubiak, *J. Am. Chem. Soc.* **2014**, *136*, 14598–14607.
[68] X.-Q. Zhu, M.-T. Zhang, A. Yu, C.-H. Wang, J.-P. Cheng, *J. Am. Chem. Soc.* **2008**, *130*, 2501–2516.
[69] Y. Zhang, T. S. Lee, J. L. Petersen, C. Milsmann, *J. Am. Chem. Soc.* **2018**, *140*, 5934–5947.
[70] S. Chardon-Noblat, S. Cosnier, A. Deronzier, N. Vlachopoulos, *J. Electroanal. Chem.* **1993**, *352*, 213–228.
[71] S. Fukuzumi, T. Kobayashi, T. Suenobu, *Angew. Chem. Int. Ed.* **2011**, *50*, 728–731; *Angew. Chem.* **2011**, *123*, 754–757.
[72] Y. Hayashi, S. Kita, B. S. Brunschwig, E. Fujita, *J. Am. Chem. Soc.* **2003**, *125*, 11976–11987.

Manuscript received: February 10, 2021
Revised manuscript received: March 13, 2021
Accepted manuscript online: March 17, 2021
Version of record online: May 2, 2021